

Supplemental Materials

Molecular testing

Tumor tissue was macro-dissected from formalin-fixed paraffin embedded (FFPE) tissue sections. Tumor purity was estimated at 90%. Tumor DNA and RNA were extracted from FFPE slides using the AllPrep DNA/RNA mini kit (Qiagen). DNA was also extracted from matched peripheral blood. Genetic testing comprised the targeted analysis of 2.34 Mb genomic regions implicated in cancer, including sequencing of the entire coding regions of 386 genes. Single nucleotide variants were detected using combined VarScan (1), Mutect (2) and ugSomatic (3) variant callers. Copy number variations were detected using an in-house platform (manuscript in preparation). Structural variants were identified using GRIDSS (4) and mutation signatures were analyzed as described by Alexandrov et al (5).

Tumor RNA was subjected to Anchored Multiplex PCR (AMP) analysis (6) using the Archer FusionPlex™ Oncology Research Panel following the manufacturer's instructions. AMP results were analysed using the Archer Analysis 5.1 pipeline which provides simultaneous detection of gene fusions and relative expression of target genes. The relative expression of genes in the Archer FusionPlex panel was normalized against the 4 housekeeping control genes *CHMP2A*, *GPI*, *RAB7A* and *VCP*. Tumor RNA was also used for RT-PCR followed by Sanger sequencing using the following primers:

GOLGA4 Ex20F: 5'-AACAACTGTGGGGACACCTT-3'

RAF1 Ex9R: 5'-CCTGTTGGGCTCAGATTGTT-3'

Histology and Immunohistochemistry analysis

FFPE sections of tumor tissues were stained with hematoxylin and eosin (H&E) for histological assessment. Diagnostic IHC was performed using kits following the

manufacturers' instructions but briefly, the following primary antibodies were used on a Ventana Benchmark Ultra autostainer at previously optimized dilutions; mouse monoclonal anti-Melan-A (A103, Leica Biosystems, NCL-L-MelanA) 1:50, rabbit polyclonal anti-S100 (Agilent Technologies, Z0311) 1:3000, mouse monoclonal anti-SOX10 (BC34, Biocare Medical, ACI3099C) 1:50, mouse monoclonal anti-HMB-45 (HMB-45, Agilent Technologies, M0634) 1:400, mouse monoclonal anti- β -catenin (17C2, Leica Biosystems, NCL-L-B-CAT) 1:50, rabbit monoclonal anti-Ki67 (30-9, Ventana Medical Systems, 790-4286) RTU, mouse monoclonal anti-CD163 (MRQ-26, Cell Marque) and rabbit monoclonal anti-cyclin D1 (SP4, Spring Bioscience, M3044) 1:50. All protocols used Cell Conditioning 1 (CC1) heat antigen retrieval buffer and visualization by OptiView DAB IHC Detection Kit (Ventana Medical, 950-124 and 760-700). Mouse monoclonal anti RAF-1 (E-10, Santa Cruz Biotechnology INC. sc-7267) and rabbit monoclonal anti-phospho-ERK (ERK1/2 Thr202/Tyr204 Cell Signaling, #4370), were performed manually and using a Dako Autostainer respectively as follows, antigen unmasking done using Dako High pH retrieval buffer (Agilent Technologies GV80411) at 98oC for 20 minutes in a Dako PT Link and 125oC, 15-18PSI pressure cooker, antibody incubation at a working dilution of 1:10 at 4oC overnight and 1:200 for 60 minutes at room temperature, visualization was completed for both antibodies using Dako Envision Flex kit (Agilent Technologies GV80011). All sections were briefly counter stained using Mayer's Hematoxylin, blued in Scott's tap water, dehydrate and mount performed on a Dako Autostainer.

Fluorescence In Situ Hybridization

Formalin-fixed paraffin-embedded sections were de-waxed, heat-treated at 124°C for 3 minutes in invitrogen Heat Tissue Pretreatment Solution (pH 7.0) with a DakoCytomation Pascal Pressure Chamber, washed in distilled water for 3 minutes, then digested with invitrogen Digest-All 3 (Pepsin Solution) at room temperature (RT) for 20 minutes. Slides

were then washed, dehydrated, air dried then 10 microlitres of RAF1 break apart probe (Empire Genomics, catalog #RAF1-20-ORGR) was placed onto the area of interest. Slides were then denatured at 85°C for 5 minutes with a Dako Hybridizer and then hybridized at 37°C for a minimum of 14 hours. Slides were washed with 2XSSC/0.1% TERGITOL™ solution (Type NP-40) at RT for 5 minutes and 2XSSC/0.3% TERGITOL™ solution at 73°C ± 1°C for 2 minutes, then air-dried, counterstained with 10µL of VECTASHIELD® Antifade Mounting Medium with DAPI and coverslipped. Cells were considered positive (rearranged) if there was a split one or more signal widths apart between the 5' and 3' signals. Digital FISH images were captured using a ZEISS AXIO Imager.Z2 Upright Microscope with Isis Fluorescence Imaging (the 3' orange signal was false colored red).

NanoString analysis of gene expression

Gene expression counts were obtained using a custom codeset on the nCounter system (NanoString Technologies) according to the manufacturer's protocol. Hybridisation reactions were performed at 65°C for 16-18 hours with 300ng of total RNA, reporter and capture probes. Transcript count data was normalised and log₂ transformed using the R package NanoStringNorm (7) against five housekeeping control genes TRIM39, EIF2B4, ERCC3, PRPF38A and ZNF143 and a reference set of 148 primary and metastatic tumors of various types. Candidate oncogenes expressed at levels greater or less-than two standard deviations from the mean of a pan-cancer reference set (N = 148) and a melanoma-specific reference set (N = 11) (Z-scores of ≥ 2 or ≤ -2) were considered as highly over- or underexpressed, while Z scores of between 1 and 2 or -1 and -2 were considered as moderately over- or underexpressed. Z scores between 1 and -1 were considered unchanged.

Therapeutic decisions

Treatment with combination Ipilimumab (IPI) and Nivolumab (NIVO) has shown an improvement in overall survival at 5 years regardless of PD-L1 staining (8). In addition, an analysis of three clinical trials (Checkmate 069, Checkmate 066, Checkmate 067) indicated that patients with PD-L1 expression of < 5% PD- L1 (low) appear to have a great benefit from combination compared with single agent therapy. Overall response rate [ORR] is high to combination IPI + NIVO (54.9%) v NIVO (39.7%). In those patients with higher (>5% tumour PD-L1) the difference in ORR is less pronounced (68.5% vs 59.0%) (9).

Trametinib was initially chosen as a single agent MEK inhibitor. Trametinib has a well-established safety profile in the treatment of melanoma, particularly in those patients with NRAS mutations and atypical BRAF alterations (10-12).

Trametinib and cobimetinib have not been compared in a head to head trial. Both drugs are small molecule orally administered inhibitors of both MEK1 and MEK2. Trametinib is a reversible, highly selective allosteric inhibitor of MEK1/MEK2 activation and kinase activity, with a half-maximum inhibitory concentration (IC₅₀) of 0.7–0.9 nmol/L. Cobimetinib is a potent, allosteric and highly selective MEK1/2 inhibitor, with a biochemical (IC₅₀) of 0.9 nM against MEK. The dosing schedule between the two drugs varies, with trametinib administered at 2mg daily continuous dosing and cobimetinib 60mg daily for 21 days of a 28-day cycle and their side effect profile is slightly different (13, 14). The patient commenced on treatment with immunotherapy following seven weeks of single agent MEK inhibition.

Dermal metastasis

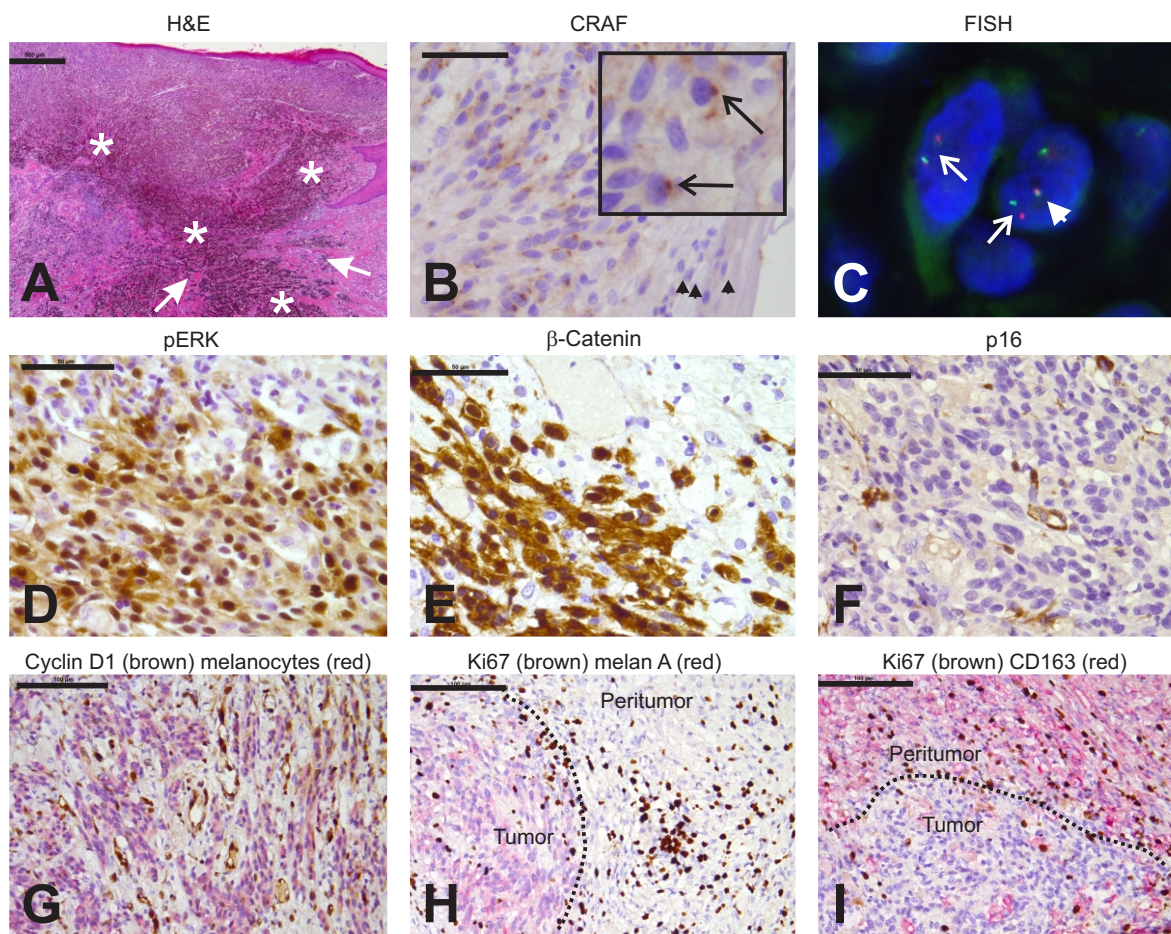
A dermal metastasis was excised from the patient on day 190, 28 days after the commencement of the MEKi. It showed histological hallmarks typical for regression including dense infiltrates of pigmented macrophages (melanophages) and lymphocytes, as well as foci of established fibrosis (Supp. Figure 1A). We detected *GOLGA4-RAF1* mRNA by RT-PCR/Sanger sequencing in this tumor and paranuclear CRAF expression (Supp. Figure 1B).

Interestingly, only ~1-2 copies of *RAF1* per tumor nucleus were detected by FISH (Supp. Figure 1C), compared to 5-10 copies per nucleus in the nodal metastasis (Figure 3K). The dermal tumor cells showed strong expression of β -catenin and pERK, and lacked p16 expression, similar to the nodal metastasis (Supp. Figure 1D-F). Cyclin D1 was intensely expressed in endothelial cells and Ki67 index was high in the infiltrating melanophages and lymphocytes. However, in contrast to their high expression in the nodal metastasis, cyclin D1 expression and the Ki67 index were low in dermal tumor cells (Supp. Figure 1G-I). The low tumor cell proliferative activity and morphological features of tumor regression are likely to be due to the MEKi treatment. The maintenance of high levels of pERK and low copy number of rearranged *RAF1* are intriguing. They possibly represent a selection of a MEK-independent process. Unfortunately, we could not explore this further as we were unable to obtain tissue from a bona fide MEKi-refractory tumor focus later in the disease time course.

Supplementary References

1. Koboldt DC, Chen K, Wylie T, Larson DE, McLellan MD, Mardis ER, et al. VarScan: variant detection in massively parallel sequencing of individual and pooled samples. *Bioinformatics*. 2009;25(17):2283-5.
2. Cibulskis K, Lawrence MS, Carter SL, Sivachenko A, Jaffe D, Sougnez C, et al. Sensitive detection of somatic point mutations in impure and heterogeneous cancer samples. *Nat Biotechnol*. 2013;31(3):213-9.
3. Rosenthal R, McGranahan N, Herrero J, Taylor BS, and Swanton C. DeconstructSigs: delineating mutational processes in single tumors distinguishes DNA repair deficiencies and patterns of carcinoma evolution. *Genome Biol*. 2016;17:31.
4. Cameron DL, Schroder J, Penington JS, Do H, Molania R, Dobrovic A, et al. GRIDSS: sensitive and specific genomic rearrangement detection using positional de Bruijn graph assembly. *Genome Res*. 2017;27(12):2050-60.
5. Alexandrov LB, Nik-Zainal S, Wedge DC, Aparicio SA, Behjati S, Biankin AV, et al. Signatures of mutational processes in human cancer. *Nature*. 2013;500(7463):415-21.
6. Zheng Z, Liebers M, Zhelyazkova B, Cao Y, Panditi D, Lynch KD, et al. Anchored multiplex PCR for targeted next-generation sequencing. *Nat Med*. 2014;20(12):1479-84.
7. Waggott D, Chu K, Yin S, Wouters BG, Liu FF, and Boutros PC. NanoStringNorm: an extensible R package for the pre-processing of NanoString mRNA and miRNA data. *Bioinformatics*. 2012;28(11):1546-8.
8. Long GV, Larkin J, Ascierto PA, et al. PD-L1 expression as a biomarker for nivolumab (NIVO) plus ipilimumab (IPI) and NIVO alone in advanced melanoma (MEL): A pooled analysis. *Annals of Oncology*. 2016;27(suppl_6):1112PD.

9. Callahan MK, Kluger H, Postow MA, Segal NH, Lesokhin A, Atkins MB, et al. Nivolumab Plus Ipilimumab in Patients With Advanced Melanoma: Updated Survival, Response, and Safety Data in a Phase I Dose-Escalation Study. *J Clin Oncol*. 2018;36(4):391-8.
10. Falchook GS, Lewis KD, Infante JR, Gordon MS, Vogelzang NJ, DeMarini DJ, et al. Activity of the oral MEK inhibitor trametinib in patients with advanced melanoma: a phase 1 dose-escalation trial. *Lancet Oncol*. 2012;13(8):782-9.
11. Kim KB, Kefford R, Pavlick AC, Infante JR, Ribas A, Sosman JA, et al. Phase II study of the MEK1/MEK2 inhibitor Trametinib in patients with metastatic BRAF-mutant cutaneous melanoma previously treated with or without a BRAF inhibitor. *J Clin Oncol*. 2013;31(4):482-9.
12. Thota R, Johnson DB, and Sosman JA. Trametinib in the treatment of melanoma. *Expert Opin Biol Ther*. 2015;15(5):735-47.
13. Rosen LS, LoRusso P, Ma WW, Goldman JW, Weise A, Colevas AD, et al. A first-in-human phase I study to evaluate the MEK1/2 inhibitor, cobimetinib, administered daily in patients with advanced solid tumors. *Invest New Drugs*. 2016;34(5):604-13.
14. Infante JR, Fecher LA, Falchook GS, Nallapareddy S, Gordon MS, Becerra C, et al. Safety, pharmacokinetic, pharmacodynamic, and efficacy data for the oral MEK inhibitor trametinib: a phase 1 dose-escalation trial. *Lancet Oncol*. 2012;13(8):773-81.



Supplemental Figure 1. Expression of key MAPK, WNT and cell cycle proteins in the dermal metastasis. (A) H&E stain of dermal metastasis. Arrows show fibrosis, asterisks show dense infiltrates of melanophages (B) IHC for CRAF in dermal metastasis. Arrows show strong paranuclear staining (insert). There is no expression in the epidermal (arrowhead) and stromal (double arrowhead) cells adjacent to the dermal tumor. (C) Breakapart RAF1 FISH in tumor cells. Note the widely separated 5' (green, centromeric) and 3' (red, telomeric) signals in tumor cells (arrows). A fused 5' and 3' signal is shown for comparison (arrowhead). (D, E) IHC for pERK (D) and β -catenin (E) showing nuclear staining and cytoplasmic staining in tumor cells. (F) IHC for p16 showing no staining in tumor cells (the occasional positive staining is in stromal cells). (G) IHC for cyclin D1 (brown) and melan-A (red) showing low cyclin D1 expression in tumor cells and high expression in endothelial cells. (H) IHC for Ki67 (brown) and melan-A (red) showing low numbers of Ki67-positive tumor cells and high numbers of Ki67-positive peritumoral cells. (I) IHC for Ki67 (brown) and CD163 (red) showing low numbers of Ki67-positive tumor cells and high numbers of Ki67-positive peritumoral macrophages. Scale bar = 200 μ m (A) and 50 μ m (B, D-I). NB. CD163 clone MRQ-26 (Cell Marque).